Chapter 5
Expanding Single Frequency Excitations to Piecewise Bandwidth Excitations for Low Speed Cameras Vision-based vibration Measurements

Davide Mastrodicasa, Andrea Sabatini, Emilio Di Lorenzo, Bart Peeters, and Patrick Guillaume

Abstract Mechanical products in industries such as automotive and aerospace are tested for validation using vibration measurements and experimental modal analysis. These tests are usually carried out using pointwise sensors connected to the structure. Image processing techniques like Digital Image Correlation (DIC) are developed to perform modal analysis. One area where DIC is of interest is in the use of cheap, light, and low-speed cameras for detecting the high-frequency behavior of structures. This work focuses on the use of signal reconstruction algorithms for bandlimited signals, which makes it possible to go beyond the Nyquist Shannon frequency limit even without the use of high-speed cameras. The approach involves exciting a structure using a band-limited signal, reconstructing the output, and performing modal analysis. A numerical validation of the approach has been conducted on a simple simulated MDOF system. An experimental validation has been conducted on a simple cantilever beam.

Keywords DIC · Modal Analysis · Vibration Analysis · Low-speed cameras · Down-sampling

Introduction

Experimental Modal Analysis (EMA) is an important technology used to study structural dynamics. It breaks down complex phenomena into separate modes, which reveal natural frequencies, modal damping, and mode shapes [1]. These modes provide insights into the dynamic properties of structures and are derived from controlled forced vibrations and natural ambient vibrations [2–4]. Together, these modal parameters form a Modal Model that is crucial for various applications, from automotive to aerospace industries. It helps in the design, optimization, and validation of Finite Element (FE) models.

Traditionally, EMA requires measuring system responses through point-wise sensors like accelerometers. However, this can be labor-intensive and introduce electrical noise [5]. Vision-based methods, such as Digital Image Correlation (DIC), are becoming increasingly popular because they enable full-field 3D measurements with high accuracy. DIC was traditionally used for static measurements but has now expanded into dynamic analysis. Phase-based Motion Magnification (PMM) and Lucas–Kanade (LK) optical flow offer similar approaches. Additionally, deep learning techniques are employed to predict displacements and strains, which outperform traditional methods in terms of computational time. These non-contact vision-based methods are useful in Structural Health Monitoring (SHM) in various fields, from aeroelasticity to wind energy and aerospace.

However, measuring high-frequency displacements presents challenges due to camera speed and resolution limitations. Recent advancements extend the use of low-speed cameras and down-sampling methods to accommodate the use of low-speed cameras for high-frequency measurements [6–7]. This paper presents a novel data acquisition and post-processing

Davide Mastrodicasa · Andrea Sabatini · Emilio Di Lorenzo · Bart Peeters
Siemens Industry Software NV, Interleuvenlaan 68, Leuven, 3001, Belgium
e-mail: davide.mastrodicasa@siemens.com; andrea.sabatini.ext@siemens.com; emilio.dilorenzo@siemens.com; bart.peeters@siemens.com

Davide Mastrodicasa · Patrick Guillaume
Vrije Universiteit Brussel, Pleinlaan 2, Brussels, 1050, Belgium
e-mail: davide.mastrodicasa@siemens.com; patrick.guillaume@vub.be

Janko Slavic et al. (eds.), *Computer Vision & Laser Vibrometry, Vol. 6*, Conference Proceedings
of the Society for Experimental Mechanics Series, https://doi.org/10.13052/97887-438-0151-1_5

strategy to reconstruct high-frequency measurement responses without the need for single harmonic excitation.

This approach is numerically validated on an MDOF system. After, the methodology is applied on a simple cantilever beam, and validated against accelerometer data.

Background

A bandlimited continuous-time signal $x(t)$ in the bandwidth $B = F_H - F_L$ Hertz can be uniquely recovered from its samples provided that the sampling rate $f_s \geq 2B$ Hz. This chapter illustrates two different methods of signal reconstruction for a bandlimited down-sampled signal.

- The first method (Interpolation method) exploits the reconstruction process in the time domain.
  A signal $x(t)$ can be recovered in the time domain from its down-sampled version $x(nT_s)$ using the equation:

$$x(t) \approx \sum_n x(nT_s) \bullet g(t - nT_s)$$

  where $g(t) = \frac{\sin(\pi Bt)}{\pi Bt} \cos(2\pi F_c t)$ and Fc is the central frequency of the band B calculated as $F_c = \frac{(F_L + F_H)}{2}$
- The second method (repMat method) instead makes use of the concept of frequency shift without reconstructing the signal $x(t)$ in the time domain. Any bandpass signal $x(t)$, having a Fourier transform $X(f)$, can be represented by an equivalent lowpass signal $x_l(t)$, having a Fourier transform $X_l(f)$ whose relation with $X(f)$ is given by the equation:

$$X_l(f) = X(f + F_c)$$

  which means that the spectrum of the bandpass signal $x(t)$ can be obtained from the spectrum of the complex signal $x_l(t)$ by a frequency translation of a known quantity. The concept behind this approach is shown in Figure 1.

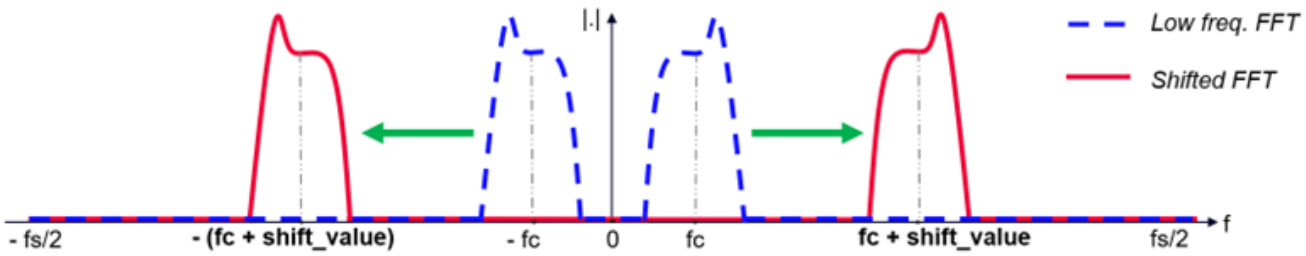

Fig. 1 Frequency Shift concept of a bandlimited spectrum.

These two methods are analyzed separately and a numerical validation over a generic bandlimited signal such as chirp or pseudorandom is performed.

Numerical Validation

Numerical validations have been conducted on a multi-degree of freedom system, shown in Figure 2. The model is built with the following parameters: $k = 900\ kN/m$; $m = 50\ kg$; $m_3 = 20\ kg$; $c = 10\ Ns/m$; $f_1 = f_2 = 0$; $f_3 = Chirp(50 - 75)\ Hz$.

To validate the methodology, the response x_2 is computed with a sampling frequency $f_{ori} = 800$ Hz (black signal). The x_2 signal is down-sampled reducing the sampling frequency to $f_{ds} = 50$ with respect to the constraint of $f_{ds} \geq 2B = 2(f_H - F_L) = 50$ Hz (red signal). Finally, the Interpolation method previously introduced is used to reconstruct the original signal and to compare the reconstruction with it (green signal).

This approach shows high fidelity of the reconstructed data, showing TRAC/FRAC values higher than 99% and a PAC value of 79%.

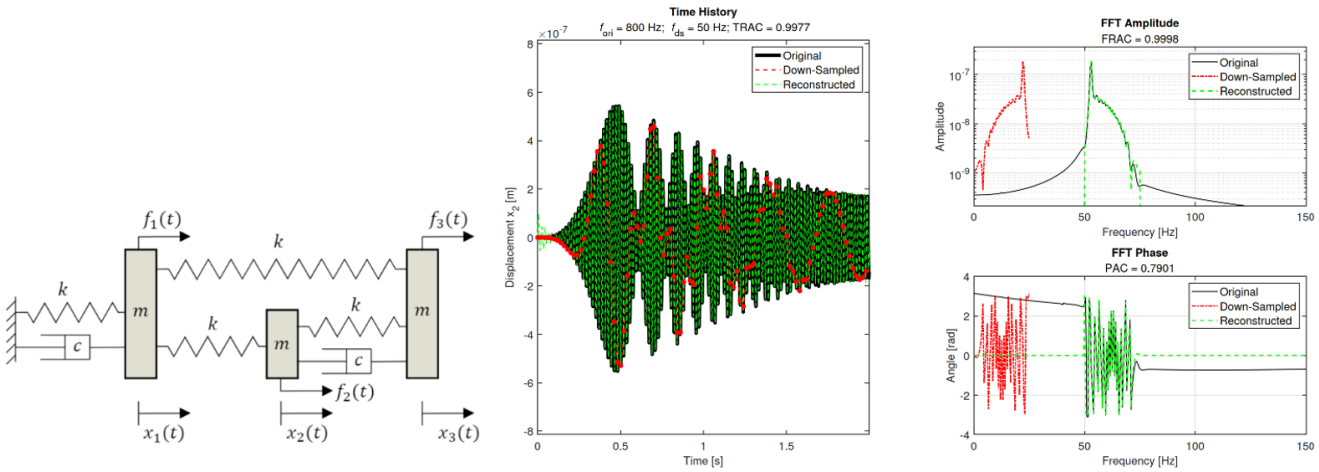

Fig. 2 MDOF Validation. left) MDOF model. right) Original-Down sampled-Reconstructed Signal using the Interpolation method.

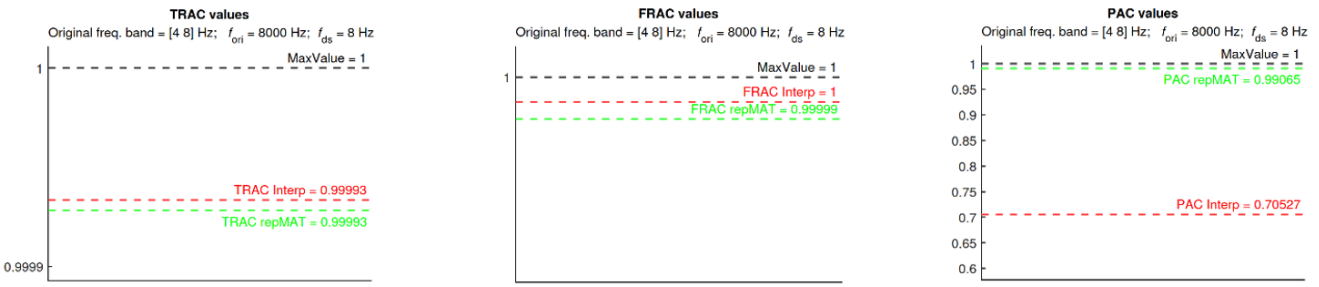

Fig. 3 TRAC/FRAC/PAC for Interpolation method and repMat method reconstruction Chirp Excitation F_L =4 Hz; F_H =8 Hz.

The same model has been used to make a comparison between the Interpolation method and the RepMat method in the frequency band $[4-8]$ Hz shows a good agreement between the two methodologies, as shown in Figure 3.

In Figure 3, it is clear that there is good agreement between the two methodologies regarding the TRAC and the FRAC. However, there is a difference in the PAC, favoring the RepMat approach. Therefore, this methodology has been used in the experimental validation.

Experimental Validation

The experimental validation was carried out on a cantilever beam (400×40×5 mm) excited by using an electrodynamic shaker in multiple sub-bands in the frequency range $[0-820]$ Hz. The different sub-bands are reconstructed using the RepMat approach. The full experimental setup, including two 5 MPx cameras, the lights, and the SCADAS acquisition systems, is shown in Figure 4.

The structure was also instrumented with 1 load cell to compute the FRFs and 10 accelerometers to validate the proposed camera-based approach.

In the test case, 40 sub-bands of around 40 Hz overlap with each other by 50%. The purpose is to cover the global range $[0\ 820]$ Hz, including all five modes identified in a preliminary accelerometer test.

The measuring phase involves the acquisition of the input force via the force cell (useful to compute the FRF for the modal analysis in post-processing), the accelerations via the 10 accelerometers, and the down-sampled displacements via the cameras by using DIC. After the measuring phase where all the needed data are collected, in the post-processing phase all the down-sampled displacements are reconstructed in the frequency domain via the application of the RepMat algorithm.

Now that the displacement signals are reconstructed the computation of the FRF can be computed by using the H_1 estimator:

$$H_1 = \frac{G_{XF}}{G_{FF}} = \frac{X(f)F^*(f)}{F(f)F^*(f)}$$

where $X(f)$ the FFT of the reconstructed displacements and $F^*(f)$ the FFT complex conjugate of the input force.

Fig. 4 Experimental Setup.

As mentioned above, a preliminary test was conducted on the beam to investigate its dynamic behavior and understand the modes targeted by the reconstruction approach.

Figure 5 shows the FRF sum of the 10 accelerometers and the characterized mode shapes.

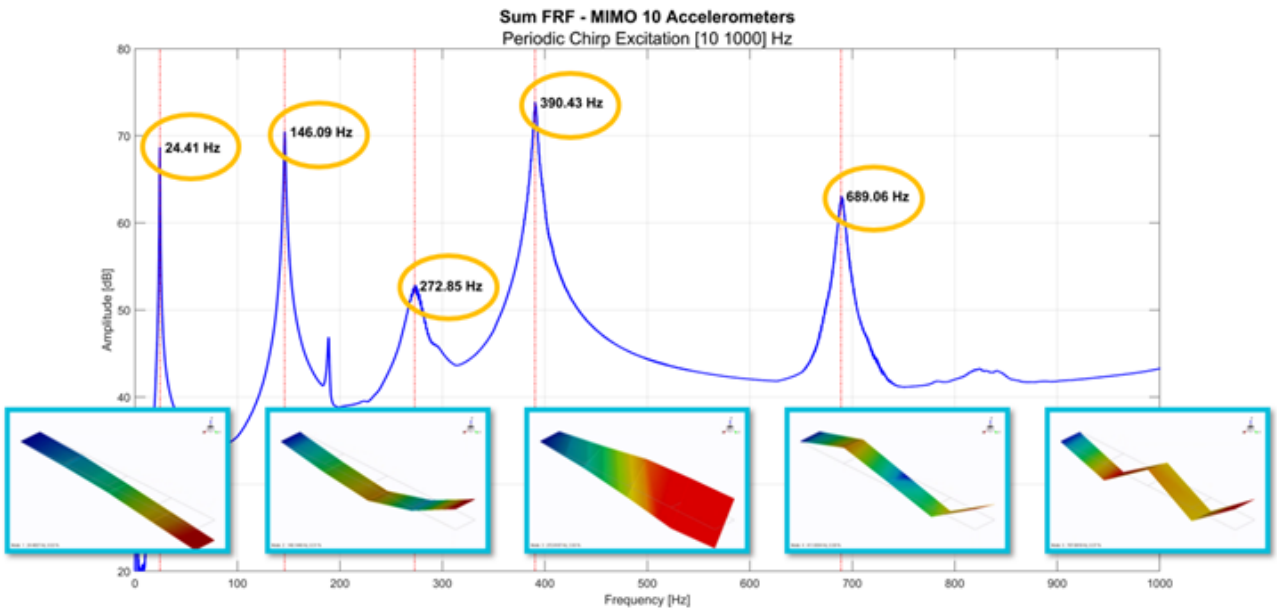

Fig. 5 FRF Sum of the preliminary test and the computed mode shapes.

Knowing the location of the modes helps in choosing some target bands to be analyzed for the reconstruction. Successively all the 40 sub-bands will be analysed for assembling all the tests in a unique FRF.

The results of the modal analysis procedure on 3 of the 40 sub-bands are shown in Figure 6 together with the estimated DIC mode-shapes.

For each frequency band, two FRFs are calculated: one representing the sum of the FRFs from the 10 accelerometers (denoted by the red line), and another representing the sum of the FRFs from the 2123 points of the DIC reconstructed displacements (denoted by the blue line). Additionally, an integrated FRF derived from the accelerometers is displayed (shown as the light blue line). The degree to which the light blue line (i.e., the integrated accelerometer FRF) aligns with the blue line (i.e., the FRF from reconstructed displacements) indicates the accuracy of the procedure. A high level of overlap

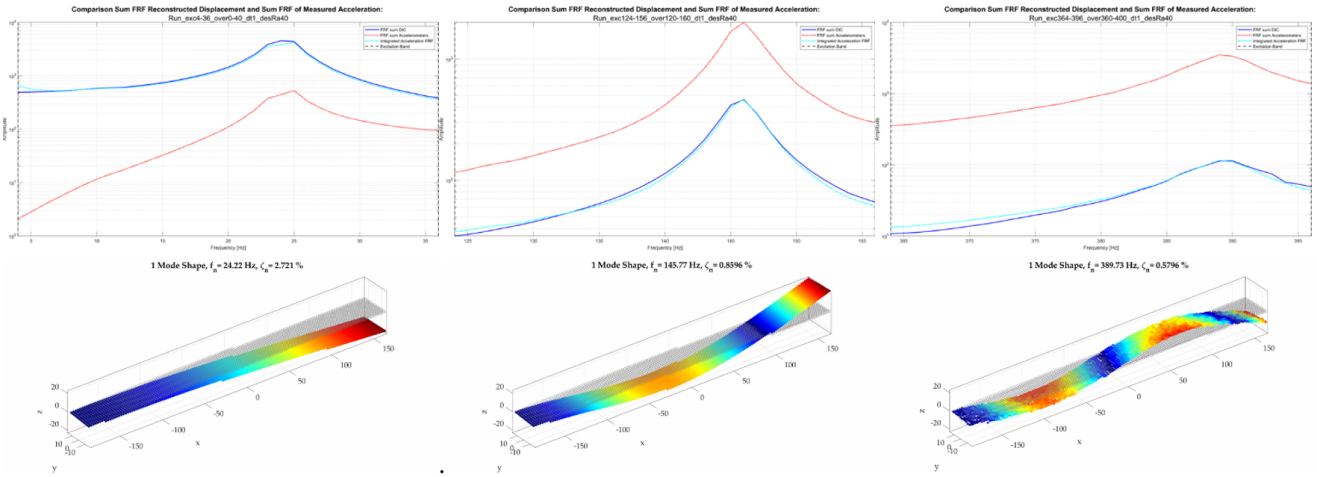

Fig. 6 Experimental Validation in the frequency bands left) 4-36 Hz center) 124-156 Hz right) 364-396 Hz.

suggests that comparable FRF data are obtained using both the accelerometer measurements and the low-speed cameras in conjunction with the reconstruction method. Furthermore, for each band, the mode shapes output from the PolyMax algorithm are also presented.

A general dynamic procedure for FRF branch assembly has been developed, consisting of the following steps:

1. Loading of FRFs and Coherences: Load the FRFs and Coherence functions for all frequency bands under consideration.
2. Segmentation of FRF and Coherence: Segment the FRF and Coherence data based on the excitation conditions.
3. Identification of Overlap Zones: Identify the overlapping regions between different frequency bands.
4. Selection of Optimal Coherence Branches: Within the overlap zones, select the branches that exhibit the best Coherence.
5. Concatenation of All Branches: Assemble the selected branches to form a continuous FRF across all bands.

Figure 7 illustrates the simultaneous loading of all the FRF and coherence results across the 40 frequency bands. It is important to note that the FRF data should be analyzed within the corresponding excitation band to ensure accuracy and relevance to the dynamic response under study.

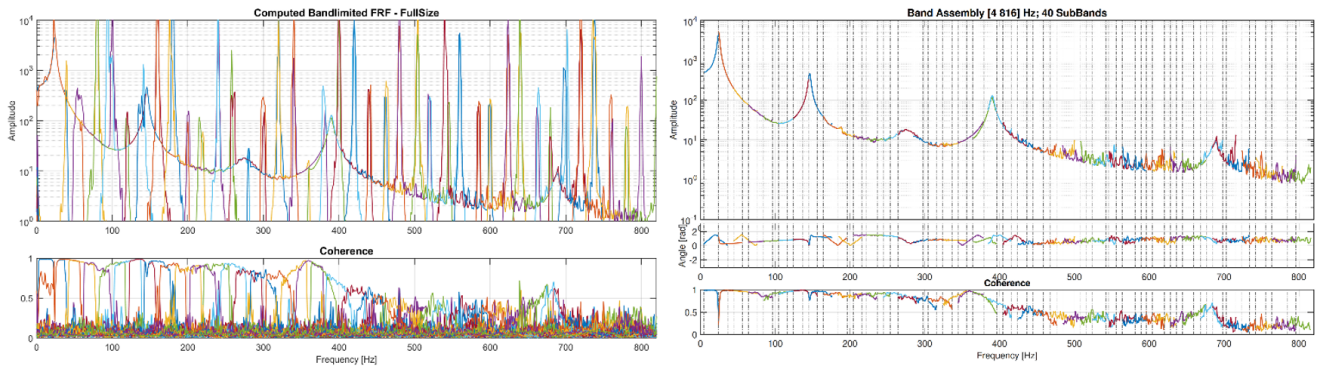

Fig. 7 left) Loaded FRFs and Coherences of the chosen bands right) FRFs and Coherences considered only in the excitation frequency range.

Figure 7 (right) presents the results obtained by selecting the specific FRF branches for each band within the excitation range, effectively ”cleaning” the plot shown in Figure 7 (left). Additionally, Figure 7 (right) displays the phase of the FRF, where the phase trend reveals inversions corresponding to the resonance peaks. However, the phase does not always transition smoothly, unlike the amplitude, particularly at frequencies around 50 Hz, 200 Hz, and 370 Hz. These discontinuities in the phase may affect the accuracy of the PolyMax algorithm. The underlying causes of the imperfect phase transitions

remain unclear and require further investigation. Moreover, the overall upward trend in the phase could indicate imperfect synchronization between the excitation force and the system's response. At higher frequencies, coherence decreases, leading to noisy FRF data in both amplitude and phase.

Conclusion

This study provided an in-depth analysis of the implementation and development of reconstruction algorithms for down-sampled displacements, using DIC for vibration measurements. The methodology enabled high-frequency measurements using low-speed cameras while achieving higher resolution.

Key accomplishments include:

- The development and numerical validation of two reconstruction algorithms, tested on simple signals and a simulated MDOF system.
- Validation of experimental results using accelerometer sensors.
- Creation of a dynamic and parametric FRF assembly algorithm for modal analysis after collecting data from band-limited runs.
- Successful PolyMax analysis, yielding accurate mode shapes comparable to those obtained with accelerometers.

Future improvements should focus on reducing post-processing time, particularly by developing systematic and iterative scripts to streamline the workflow. Further investigation is needed to address the noise at higher frequencies, including validation with high-speed cameras and testing on more complex structures. Overall, the approach demonstrated promising results in capturing the full dynamics of a structure with low-speed cameras, reducing the need for contact sensors and managing smaller datasets.

References

1. B. Peeters, H. Van der Auweraer, P. Guillaume, J. Leuridan, The polymax frequency-domain method: A new standard for modal parameter estimation?, Shock and Vibration 11 (2004) 395–409.
2. C. Pappalardo, D. Guida, System identification and experimental modal analysis of a frame structure, Engineering Letters 26 (2018) 56–68.
3. H. Van der Auweraer, Structural dynamics modeling using modal analysis: applications, trends and challenges, in: IMTC 2001. Proceedings of the 18th IEEE Instrumentation and Measurement Technology Conference. Rediscovering Measurement in the Age of Informatics (Cat. No.01CH 37188), volume 3, 2001, pp. 1502–1509 vol.3. doi:10.1109/IMTC.2001.929456.
4. A. Cusano, P. Capoluongo, S. Campopiano, A. Cutolo, M. Giordano, F. Felli, A. Paolozzi, M. Caponero, Experimental modal analysis of an aircraft model wing by embedded fiber bragg grating sensors, IEEE Sensors Journal 6 (2006) 67–77.
5. A. Zanarini, Full field optical measurements in experimental modal analysis and model updating, Journal of Sound and Vibration 442 (2019) 817–842.
6. J. Baqersad, P. Poozesh, C. Niezrecki, P. Avitabile, Photogrammetry and optical methods in structural dynamics – a review, Mechanical Systems and Signal Processing 86 (2017) 17–34. Full-field, non-contact vibration measurement methods: comparisons and applications.
7. Paolo Neri. Frequency-band down-sampled stereo-DIC: Beyond the limitation of single frequency excitation. Mechanical Systems and Signal Processing, 172:108980, June 2022.